Available online at www.sciencedirect.com
SCIENCE DIRECT®
ELSEVIER
Journal of Magnetism and Magnetic Materials 263 (2003) L1–L9
journal of magnetism and magnetic materials
www.elsevier.com/locate/jmmm

Letter to the Editor

On the computation of the demagnetization tensor field for an arbitrary particle shape using a Fourier space approach

M. Beleggia[a], M. De Graef[b,*]

[a] *Materials Science Department, Brookhaven National Laboratory, Upton, NY 11973, USA*
[b] *Department of Materials Science and Engineering, Carnegie Mellon University, Pittsburgh, PA 15213-3890, USA*

Received 20 January 2003; received in revised form 25 February 2003

Abstract

A method is presented to compute the demagnetization tensor field for uniformly magnetized particles of arbitrary shape. By means of a Fourier space approach it is possible to compute analytically the Fourier representation of the demagnetization tensor field for a given shape. Then, specifying the direction of the uniform magnetization, the demagnetizing field and the magnetostatic energy associated with the particle can be evaluated. In some particular cases, the real space representation is computable analytically. In general, a numerical inverse fast Fourier transform is required to perform the inversion. As an example, the demagnetization tensor field for the tetrahedron will be given.

PACS: 41.20.Gz; 75.30.Gw; 75.40.Mg

Keywords: Demagnetization tensor field; Shape amplitude; Tetrahedron; Magnetometric demagnetization tensor; Demagnetization energy

1. Introduction

The calculation of the demagnetizing tensor N_{ij} is of fundamental importance for a quantitative analysis of the energy associated with a particular magnetization state of a magnetized particle. All micromagnetic simulations rely on the numerical evaluation of N_{ij}, often with strong assumptions about the geometry of the cell. A complete theoretical scheme for the computation of the preferred magnetization direction as a function of particle shape in uniformly magnetized nanoparticles is still lacking. It is generally claimed that the analytical calculation of the demagnetizing tensor can be performed only for ellipsoidal shapes [1]; if we restrict the interest to the volume averaged demagnetizing tensor (the so-called magnetometric demagnetization factor), we can extend the computation to the cubic geometry [2]. It is the main purpose of this paper to show how we can overcome those apparent limitations, and extend the computation of N_{ij} to a much broader class of geometries, namely the faceted particles.

The shape of a particle can be described mathematically by means of the characteristic function or shape function, which is equal to unity

*Corresponding author. Tel.: +1-412-268-8527; fax: +1-412-268-7596.
E-mail address: degraef@cmu.edu (M. De Graef).

0304-8853/03/$ - see front matter
doi:10.1016/S0304-8853(03)00238-5

inside the particle and vanishes outside. It was shown in Ref. [3] how to evaluate the Fourier representation of the shape function for a faceted particle. Then, in Ref. [4], this scheme was applied to the calculation of the vector potential and electron-optical phase shift arising from a faceted magnetized particle. The Fourier space approach, recently introduced and applied to the interpretation of TEM images of semiconducting and superconducting materials [5–7], allows us to calculate the vector potential associated with the total **B**-field of the particle, which is the sum of magnetization **M** and demagnetization **H** fields. The same approach, adapted to the analysis of magnetized nanoparticles, will be employed here in order to calculate analytically the Fourier space representation of the N_{ij} tensor field.

First, the basic concepts underlying the Fourier space approach will be introduced, in particular the connection between magnetization and vector potential and the definitions of the quantities of interest. Then, to illustrate the validity of the approach, the N_{ij} tensor for a spherical particle, which is a well-known result, will be derived. Finally, to better show the opportunities opened by this approach, an example of a non-ellipsoidal particle will be given.

It is worth emphasizing that the method presented here is of general validity, and does not rely on any assumptions or simplifications. This formalism may contribute to a significant improvement of the accuracy of micromagnetic simulations, as well as lead to a new fundamental understanding of the magnetic properties of nanoparticles.

2. Theoretical model

The expression linking magnetization and magnetic vector potential,

$$\mathbf{A}(\mathbf{r}) = \frac{\mu_0}{4\pi}\int \mathbf{M}(\mathbf{r}') \times \frac{\mathbf{r}-\mathbf{r}'}{|\mathbf{r}-\mathbf{r}'|^3}\mathrm{d}^3\mathbf{r}', \tag{1}$$

represents an invaluable resource for the computation of magnetic configurations starting from a known magnetization. In fact, exploiting the convolution theorem and the linearity of the vector product operation, Eq. (1) can be written in 3D-Fourier space as ($\mathscr{F}$ represents the Fourier transform operator):

$$\mathbf{A}(\mathbf{k}) = \frac{\mu_0}{4\pi}\mathbf{M}(\mathbf{k}) \times \mathscr{F}\left[\frac{\mathbf{r}}{r^3}\right] = -\frac{\mathrm{i}\mu_0}{k^2}\mathbf{M}(\mathbf{k}) \times \mathbf{k}. \tag{2}$$

Hence, the calculation of the vector potential is reduced to a vector product, if the Fourier transform of the magnetization is computable.

In general, we can write the magnetization vector for a uniformly magnetized particle as $M_0\,\hat{\mathbf{m}}$ for $\mathbf{r}$ inside the particle, and zero outside. We introduce the dimensionless shape function $D(\mathbf{r})$ which represents the region of space bounded by the particle surface: $\mathbf{M}(\mathbf{r}) = M_0\hat{\mathbf{m}}D(\mathbf{r})$. The Fourier transform of the magnetization can be written as $M_0\hat{\mathbf{m}}D(\mathbf{k})$, where $D(\mathbf{k})$ is the Fourier transform of the shape function, often called *shape amplitude*, or *shape transform*.

From Eq. (2) we can calculate directly the Fourier space representation of the vector potential for a uniformly magnetized particle:

$$\mathbf{A}(\mathbf{k}) = -\frac{\mathrm{i}B_0}{k^2}D(\mathbf{k})(\hat{\mathbf{m}} \times \mathbf{k}), \tag{3}$$

where $\mu_0 M_0 = B_0$ is the magnetic induction corresponding to a magnetization M_0.

From the knowledge of the vector potential, one can easily calculate the magnetic induction, as $\mathbf{B} = \nabla \times \mathbf{A}$. As any differential operator in real space is a reciprocal vector in Fourier space, the nabla operator becomes $\nabla \to \mathrm{i}\mathbf{k}$. Therefore, the Curl is translated into a vector product as follows:

$$\mathbf{B}(\mathbf{k}) = \mathrm{i}\mathbf{k} \times \mathbf{A}(\mathbf{k}) = \frac{B_0}{k^2}D(\mathbf{k})(\mathbf{k} \times \hat{\mathbf{m}} \times \mathbf{k}), \tag{4}$$

which, exploiting the vector identity $\mathbf{k} \times \hat{\mathbf{m}} \times \mathbf{k} = \hat{\mathbf{m}}k^2 - \mathbf{k}(\mathbf{k} \cdot \hat{\mathbf{m}})$, and computing the inverse Fourier transform, can also be written as the sum of the induction proportional to the magnetization and the demagnetization field:

$$\begin{aligned}\mathbf{B} &= \mu_0(\mathbf{M} + \mathbf{H}) \\ &= \mu_0\mathbf{M} - \frac{B_0}{8\pi^3}\int \mathrm{d}^3\mathbf{k}\frac{D(\mathbf{k})}{k^2}\mathbf{k}(\hat{\mathbf{m}} \cdot \mathbf{k})\mathrm{e}^{\mathrm{i}\mathbf{k}\cdot\mathbf{r}}.\end{aligned} \tag{5}$$

If we define the demagnetization tensor field (note that this tensor field has also been called the *point-function demagnetization tensor* [8]) N_{ij} by the component relation: $B_i = \mu_0(M_i - N_{ij}M_j)$, then we

find an explicit expression for the tensor by comparison with Eq. (5):

$$N_{ij}(\mathbf{k}) = \frac{D(\mathbf{k})}{k^2} k_i k_j. \tag{6}$$

The real space representation, $N_{ij}(\mathbf{r})$, can be obtained by a 3D inverse Fourier transformation. The tensor field is obviously a symmetric tensor field, i.e., $N_{ij} = N_{ji}$.

This definition of N_{ij} automatically satisfies the condition that the trace of $N_{ij}(\mathbf{r})$ be equal to unity inside the particle, and vanish outside. The trace can be computed as

$$\begin{aligned}\mathrm{Tr}[N_{ij}] &= \frac{1}{8\pi^3} \int \mathrm{d}^3\mathbf{k} \frac{D(\mathbf{k})}{k^2} \sum_{i=1}^{3} k_i k_i \mathrm{e}^{\mathrm{i}\mathbf{k}\cdot\mathbf{r}} \\ &= \frac{1}{8\pi^3} \int \mathrm{d}^3\mathbf{k} D(\mathbf{k}) \mathrm{e}^{\mathrm{i}\mathbf{k}\cdot\mathbf{r}} = D(\mathbf{r}).\end{aligned} \tag{7}$$

In other words, the trace of the demagnetization tensor field is equal to the shape function. This is an important result, because it displays the connection between the demagnetization tensor field and the shape of the particle in a way that is difficult to derive from the more commonly used magnetic surface charge description; furthermore, the relation can be used to verify the numerical computation of the tensor field.

2.1. The demagnetization energy

The demagnetization energy can be derived within the Fourier space approach without involving explicitly the demagnetization tensor N_{ij}. Assuming the following definition of the magnetostatic energy:

$$E_m = -\frac{\mu_0}{2} \int_{\mathrm{V}} \mathbf{H} \cdot \mathbf{M} \, \mathrm{d}^3\mathbf{r}, \tag{8}$$

where the subscript V indicates that the integral is performed only within the particle volume, and writing the Fourier representation of the **H**-field as in Eq. (5), we obtain

$$\begin{aligned}E_m = \frac{\mu_0 M_0^2}{16\pi^3} \int_{\mathrm{V}} \left(\int \mathrm{d}^3\mathbf{k} \frac{D(\mathbf{k})}{k^2} \mathbf{k}(\hat{\mathbf{m}}\mathbf{k}) \mathrm{e}^{\mathrm{i}\mathbf{k}\cdot\mathbf{r}} \right) \\ \times \hat{\mathbf{m}} \, D(\mathbf{r}) \, \mathrm{d}^3\mathbf{r},\end{aligned} \tag{9}$$

which, after inverting the order of integration, finally yields

$$E_m = \frac{\mu_0 M_0^2}{16\pi^3} \int \mathrm{d}^3\mathbf{k} \frac{|D(\mathbf{k})|^2}{k^2} (\hat{\mathbf{m}} \cdot \mathbf{k})^2. \tag{10}$$

The last integral is obtained using $D(-\mathbf{k}) = D^*(\mathbf{k})$, which is always valid since $D(\mathbf{r})$ is a real-valued function.

Similarly, the volume average of the demagnetization tensor, the so-called magnetometric demagnetization tensor, can be computed within the Fourier space approach. It can be expressed as

$$\begin{aligned}\langle N \rangle_{ij} &= \frac{1}{V} \int_{\mathrm{V}} \mathrm{d}^3\mathbf{r} N_{ij}(\mathbf{r}) \\ &= \frac{1}{8\pi^3 V} \int \mathrm{d}^3\mathbf{k} \frac{|D(\mathbf{k})|^2}{k^2} k_i k_j.\end{aligned} \tag{11}$$

2.2. Example computation

As an example, we now compute the demagnetization tensor field for a spherical particle, for which the result is well known. The shape amplitude for the sphere is given by Beleggia [9]

$$D(\mathbf{k}) = \frac{4\pi R^2}{k} j_1(kR) \quad \text{with} \quad j_1(x) = \frac{\sin x}{x^2} - \frac{\cos x}{x}, \tag{12}$$

where $j_1(x)$ is the spherical Bessel function of first order. Substitution in Eq. (6) results in the reciprocal demagnetization tensor for the sphere:

$$N_{ij}(\mathbf{k}) = 4\pi R^5 \frac{j_1(kR)}{(kR)^3} k_i k_j. \tag{13}$$

If we scale reciprocal space by the sphere radius, $\mathbf{k}R = \mathbf{K}$, and take the inverse Fourier transform, we find for the direct space demagnetization tensor:

$$N_{ij}(\boldsymbol{\rho}) = \frac{1}{2\pi^2} \int \mathrm{d}^3\mathbf{K} \frac{j_1(\mathbf{K})}{K^3} K_i K_j \mathrm{e}^{\mathrm{i}\mathbf{K}\cdot\boldsymbol{\rho}} \tag{14}$$

with $\boldsymbol{\rho} = \mathbf{r}/R$. This integral can be expressed in spherical coordinates, using the standard expansion for the plane wave

$$\mathrm{e}^{\mathrm{i}\mathbf{K}\cdot\boldsymbol{\rho}} = 4\pi \sum_{l=0}^{\infty} \mathrm{i}^l j_l(K\rho) \sum_{m=-l}^{+l} Y_{lm}^*(\theta', \phi') Y_{lm}(\theta, \phi), \tag{15}$$

where (K,θ,ϕ) and (ρ,θ',ϕ') are the spherical coordinates corresponding to $\mathbf{K}$ and $\boldsymbol{\rho}$, respectively, and the $Y_{lm}(\theta,\phi)$ are the spherical harmonics.

The demagnetization tensor field has six independent components, which are explicitly written as

$$\begin{pmatrix} N_{11} \\ N_{22} \\ N_{33} \\ N_{12} \\ N_{13} \\ N_{23} \end{pmatrix} = -\frac{2}{\pi}\sum_{l=0}^{\infty}\sum_{m=-l}^{l} \mathrm{i}^l Y^*_{lm}(\theta',\phi') \times \int_0^{2\pi} \mathrm{d}\phi \begin{pmatrix} \cos^2\phi \\ \sin^2\phi \\ 1 \\ \cos\phi\sin\phi \\ \cos\phi \\ \sin\phi \end{pmatrix} \times \int_0^{\pi} \mathrm{d}\theta \sin\theta \begin{pmatrix} \sin^2\theta \\ \sin^2\theta \\ \cos^2\theta \\ \sin^2\theta \\ \sin\theta\cos\theta \\ \sin\theta\cos\theta \end{pmatrix} Y_{lm}(\theta,\phi) \times \int_0^{\infty} \mathrm{d}K K j_1(K) j_l(K\rho). \tag{16}$$

The angular integrals are solved easily by expressing the trigonometric functions as a linear combination of spherical harmonics and using the orthonormality of the spherical harmonics. For the radial integral we make use of the following standard integral [10, Eq. 11.4.42]:

$$\int_0^{\infty} J_{\mu}(at)J_{\mu-1}(bt)\,\mathrm{d}t = \begin{cases} \dfrac{b^{\mu-1}}{a^{\mu}} & 0<b<a, \\ \dfrac{1}{2b} & 0<b=a, \\ 0 & b>a>0, \end{cases} \tag{17}$$

where J_{μ} is a Bessel function of fractional order and we have used the relationship $j_l(x) = \sqrt{(\pi/2x)}\,J_{l+(1/2)}(x)$ between spherical Bessel functions and the Bessel-J functions.

Combining all results and reverting to the unscaled coordinate $\mathbf{r}$ in a Cartesian reference system (x,y,z), we find the following expression for the demagnetization tensor field of the sphere:

$$N_{ij}(\mathbf{r}) = H(R-r)\begin{pmatrix} \frac{1}{3} & 0 & 0 \\ 0 & \frac{1}{3} & 0 \\ 0 & 0 & \frac{1}{3} \end{pmatrix} - H(r-R) \times \frac{R^3}{3r^5}\begin{pmatrix} 3x^2-r^2 & 3xy & 3xz \\ 3xy & 3y^2-r^2 & 3yz \\ 3xz & 3yz & 3z^2-r^2 \end{pmatrix} \tag{18}$$

where $H(x)$ is the Heaviside unit step function ($H(x)=0$ for $x<0$ and 1 for $x>0$). The first term in Eq. (18) shows the well-known result that the demagnetization factor of the sphere is equal to $\frac{1}{3}$. The second-term shows that outside the sphere, the demagnetization field has dipole character. For a pure magnetic dipole of strength $\mathbf{m}$ in a sphere of vanishing radius, the magnetic induction can be computed from the demagnetization tensor as

$$\mathbf{B}(\mathbf{r}) = \mu_0\frac{3\hat{\mathbf{r}}(\hat{\mathbf{r}}\cdot\mathbf{m})-\mathbf{m}}{r^3}, \tag{19}$$

which is the standard expression for a dipole field of strength $\mathbf{m} = (R^3/3)\mathbf{M}$.

The magnetostatic energy of the uniformly magnetized sphere can be computed by combining Eqs. (10) and (12):

$$E_m = \frac{1}{2}\mu_0 M_0^2 R^3 \int \mathrm{d}^3\mathbf{K}\frac{J^2_{3/2}(K)}{K^5}(\hat{\mathbf{m}}\cdot\mathbf{K})^2. \tag{20}$$

Without loss of generality we can take $\hat{\mathbf{m}}$ along the x-direction, so that $\hat{\mathbf{m}}\cdot\mathbf{K} = K\sin\theta\cos\phi$. The angular integrals can be shown to be equal to $4\pi/3$, so that

$$E_m = \frac{2\pi}{3}\mu_0 M_0^2 R^3 \int_0^{\infty}\mathrm{d}K\frac{J^2_{3/2}(K)}{K}, = \frac{2\pi\mu_0}{9}M^2R^3. \tag{21}$$

The volume average of the demagnetization tensor field over the sphere can be computed explicitly from Eqs. (11) and (12) as

$$\langle N \rangle_{ij} = \frac{3}{4\pi} \int \mathrm{d}^3\mathbf{k} \frac{J_{3/2}^2(kR)}{k^5} k_i k_j. \tag{22}$$

Working in spherical coordinates, the angular integrals are easily shown to be equal to $(4\pi/3)\delta_{ij}$, and the remaining radial integral is given by:

$$\langle N \rangle_{ij} = \delta_{ij} \int_0^{+\infty} \mathrm{d}x \frac{J_{3/2}^2(x)}{x} = \frac{1}{3}\delta_{ij}. \tag{23}$$

3. Faceted particles

3.1. The shape amplitude

In the remainder of this paper, we will consider the case of a polyhedral particle. The magnetic properties of uniformly magnetized polyhedral particles have thus far only been investigated using numerical methods. The current interest in the properties of nanoparticles includes not only particles which have solidified or were otherwise formed into a polyhedral shape, but also intentionally shaped particles, such as patterned arrays of disks, plates, and so on. A clear understanding of the magnetic behavior of such particles requires a study of the effect of shape on the magnetization state at the nanoscale.

The polyhedral shape can be analyzed analytically, using the combination of a formalism developed by Komrska [3] and the Fourier-space approach presented here. Explicit expressions for the shape amplitude can be used to obtain an analytical expression for the demagnetizing tensor, field, and energy. Since nearly all micromagnetic simulations are performed over a mesh which can be triangular, square, hexagonal or, in general, an irregular polygon or polyhedron (for 3D simulations), it is important to be able to calculate demagnetization tensors for particle shapes which mimic the cell shapes of a micromagnetic simulation. In this section, we will first describe briefly the shape amplitude formalism. Then, a tetrahedron will be analyzed in detail.

The shape amplitude $D(\mathbf{k})$ of a polyhedral particle with E edges and F faces is given by Komrska [3]

$$D(\mathbf{k}) = -\frac{1}{k^2} \sum_{f=1}^{F} \frac{\mathbf{k}\cdot\mathbf{n}_f}{k^2 - (\mathbf{k}\cdot\mathbf{n}_f)^2} \sum_{e=1}^{E_f} L_{fe}\mathbf{k}\cdot\mathbf{n}_{fe} \times \operatorname{sinc}\left(\frac{L_{fe}}{2}\mathbf{k}\cdot\mathbf{t}_{fe}\right) \mathrm{e}^{-\mathrm{i}\mathbf{k}\cdot\boldsymbol{\xi}_{fe}^C}. \tag{24}$$

This equation is only valid if the second denominator is non-zero. If $\mathbf{k} = \pm k\mathbf{n}_f$ (in other words, if $\mathbf{k}$ is parallel to any one of the face normals), then the contribution of that particular face (or faces) must be replaced by

$$D_f(\mathbf{k}) = \mathrm{i}\frac{\mathbf{k}\cdot\mathbf{n}_f}{k^2} P_f \mathrm{e}^{-\mathrm{i}d_f\mathbf{k}\cdot\mathbf{n}_f}, \tag{25}$$

where P_f is the surface area of the face f, and d_f the distance between the origin and the face f. In the origin of Fourier space, the shape amplitude is equal to the particle volume, i.e. $D(\mathbf{0}) = V$. The symbols in Eq. (24) are illustrated in Fig. 1 and are defined as

- $\boldsymbol{\xi}_{fe}^C$ coordinate vectors of the center of the edge e of face f,
- $\mathbf{n}_f$ unit outward normal to face f,
- L_{fe} length of the eth edge of the fth face,
- $\mathbf{t}_{fe}$ unit vector along the eth edge of the fth face, defined by

$$\mathbf{t}_{fe} = \frac{\mathbf{n}_f \times \mathbf{N}_{fe}}{|\mathbf{n}_f \times \mathbf{N}_{fe}|},$$

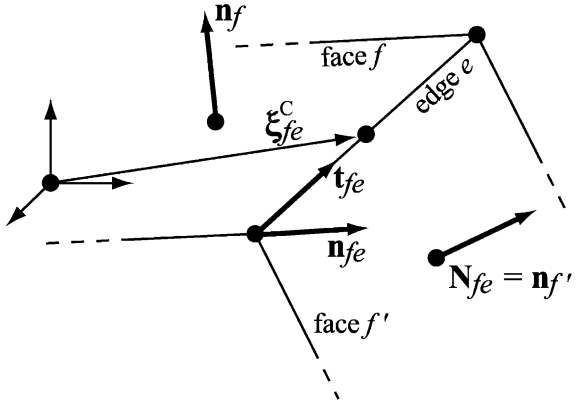

Fig. 1. Schematic representation of the face normals $\mathbf{n}_f$, edge vectors $\mathbf{t}_{fe}$, and outward edge normals $\mathbf{n}_{fe}$ used in Eq. (24).

where $\mathbf{N}_{fe}$ is the unit outward normal *on* the face which has the edge e in common with the face f,

$\mathbf{n}_{fe}$ unit outward normal *in* the face f on the edge e defined by $\mathbf{n}_{fe} = \mathbf{t}_{fe} \times \mathbf{n}_f$.

The input parameters needed to complete this computation for an arbitrary polyhedron are the N_v vertex coordinates $\boldsymbol{\xi}_v$ and a list of which vertices make up each face (counterclockwise when looking towards the polyhedron center). All other quantities can be computed from these parameters.

The shape amplitude formalism, together with Eq. (6) can be used to compute the Fourier representation of the N_{ij} tensor for an arbitrary polyhedral object with a uniform magnetization. We will illustrate the method using the tetrahedron as an example.

3.2. The Tetrahedron

The shape amplitude of the tetrahedron can be derived by inserting the vertex coordinates and various unit vectors in Eq. (24). This has been done by Komrska and Neumann [11] and the resulting expression is

$$D(\mathbf{k}) = -6V\mathrm{i}[E(a,a,a) + E(a,-a,-a) + E(-a,a,-a) + E(-a,-a,a)], \tag{26}$$

V is the volume, $a = L/\sqrt{2}$, with L the edge length of the tetrahedron, and

$$E(\alpha,\beta,\gamma) \equiv \frac{\mathrm{e}^{-\frac{\mathrm{i}}{2}(\alpha k_x + \beta k_y + \gamma k_z)}}{(\alpha k_x + \beta k_y)(\alpha k_x + \gamma k_z)(\beta k_y + \gamma k_z)}. \tag{27}$$

The lack of an inversion center causes the shape amplitude to be a complex quantity. When Eq. (26) is multiplied by $k_i k_j / k^2$, one obtains the Fourier representation of N_{ij}. This expression is exact; i.e., no approximations have been made up to this point.

Using Eq. (6), we can compute numerically the Fourier representation of N_{ij} on a discrete grid of N^3 points. Since N_{ij} is a symmetric tensor field, numerical computation involves six 3D inverse FFT (iFFT) operations on a complex function. The demagnetization tensor field has the same phase factors as the shape amplitude, so that the real space transform will be a real-valued function. One of the main disadvantages of using the discrete iFFT is the possibility of Gibbs oscillations in the real space N_{ij}, in particular since the facets of the object represent discontinuities. A direct evaluation of the inverse Fourier transform integral would circumvent this numerical problem, at the expense of significantly longer computation times. Alternatively, the Fourier space expression of N_{ij} can be multiplied by a smoothing function to eliminate the Gibbs phenomenon altogether. Furthermore, the discrete iFFT imposes periodic boundary conditions, so that the dimensions of the object with respect to the overall sampling grid must be chosen carefully. More details on the numerical techniques associated with this computation will be presented in a forthcoming paper.

The real space N_{ij} for the tetrahedron was computed on an array of 128^3 gridpoints, with the edge length L taken to be 36 grid units. Computations were carried out using single precision, complex number arithmetic on a 666 MHz Compaq TRU64 workstation. Once the tensor field is known, various 2D section can be used to represent the details. However, for a complete understanding of this tensor field, a 3D visualization is desirable. A symmetric tensor field with positive eigenvalues can be represented graphically by an array of ellipsoids. For each ellipsoid, the major axes are determined by the eigenvectors of the tensor, and the dimensions along the axes are given by the eigenvalues. Fig. 2 shows a perspective view of the demagnetization tensor field of the tetrahedron (outlined with solid cylinders); the numerical grid was sampled every eight grid points for the visualization process. All ellipsoids are inside the tetrahedron. The figure was generated by means of a raytracing program [12]; a movie, showing the entire tensor field from different viewing directions, is available from the author's website [13].

Outside the tetrahedron, the trace of the symmetric tensor vanishes, so that one or two eigenvalues must be negative. The corresponding quadratic surfaces are the single-sheet and double-sheet hyperboloids, respectively. Since these surfaces have infinite extent, it is more convenient to

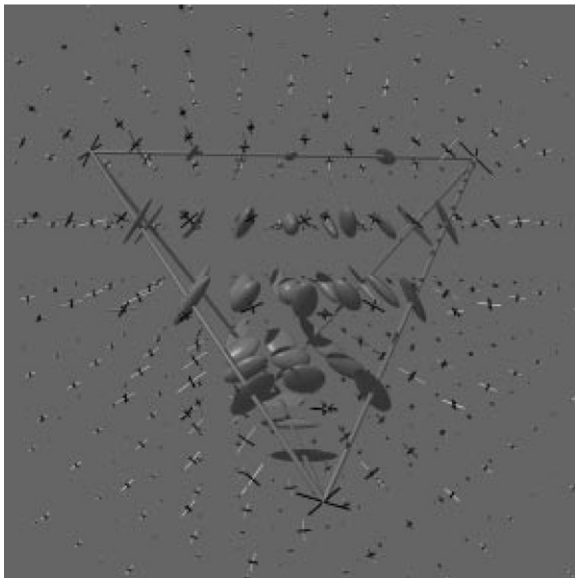

Fig. 2. Rendered perspective representation of N_{ij} for the tetrahedron. Darker ellipsoids correspond to sampling points inside the tetrahedron volume, which is outlined by thin cylinders. Outside the tetrahedron, the tensor is represented by three rods, oriented along the eigenvector directions, with lengths proportional to the modulus of the corresponding eigenvalue. The negative eigenvalue is represented by a light-colored rod.

represent only the eigenvectors and eigenvalues by means of a 3D intersection of three rods. The length of each rod corresponds to the modulus of the eigenvalues, and the orientation represents the corresponding eigenvector. Of the three rods, the lighter colored one (Fig. 2) corresponds to the negative eigenvalue; its corresponding eigenvector lies along the line connecting the grid point to the center of the tetrahedron.

This representation contains all the information needed to determine the **B**-field for an arbitrary direction of $\hat{\mathbf{m}}$. Using Eq. (5) and representing N_{ij} by its spectral decomposition, we have the following relation for the magnetic induction components:

$$B_i = B_0(m_i - C_{ij}\Lambda_{jk}\tilde{C}_{kl}m_l), \tag{28}$$

where C_{ij} is a matrix containing the eigenvectors of N_{ij} as columns, Λ_{jk} is a diagonal matrix containing the eigenvalues, and the tilde symbol indicates the transpose of a matrix. The first term in this equation is only present inside the particle volume. The interpretation of this relation is straightforward. Since the eigenvectors of a symmetric matrix form an orthonormal set, the matrix C is a unitary matrix, which means that it represents a rigid body rotation. The demagnetization field component is then determined by first rotating the unit magnetization vector into the reference frame of the ellipsoid, then multiplying component-wise with the eigenvalues, and finally rotating back to the external reference frame. This is illustrated in Fig. 3, which shows the various vectors for two different ellipsoid shapes, prolate (top row) and oblate (bottom row), and four different directions of the unit magnetization vector $\hat{\mathbf{m}}$: [0 0 1], [1 0 2], [2 0 1], and [1 0 0], using Bravais direction indices.

Near the center of the edges of the tetrahedron in Fig. 2, the demagnetization tensor corresponds to a prolate ellipsoid oriented parallel to the opposite edge. At the vertices, the ellipsoid is oblate, parallel to the opposite face. Near the center, the ellipsoids approach the spherical shape. It is clear from the figure that the point group symmetry of N_{ij} is identical to that of the tetrahedron, namely the point group $\bar{4}\mathbf{3m}$. This also follows directly from Eq. (6): the factor k_ik_j/k^2 has spherical symmetry, so when it is combined (i.e. multiplied) with the shape amplitude, the resulting expression inherits the symmetry of the shape amplitude, which is the point group of the object. Alternatively, one can view this as an application of the Neumann Principle (e.g. [14,15]): *the symmetry elements of any physical property of a crystal must include the symmetry elements of the point group of the crystal*. This can be applied to objects with a given symmetry, so that the demagnetization tensor field of a uniformly magnetized particle has the same symmetry as the particle shape.

Furthermore, if the particle has a symmetry axis of order greater than the rank of the tensor, in this case 2, then the tensor field is isotropic in a plane normal to that symmetry axis. This was shown explicitly by Moskowitz and Della Torre [8] for the particular case of the demagnetization tensor, but is valid in general for any symmetric second rank tensor. As a consequence, all particle shapes for which the point group contains multiple rotation

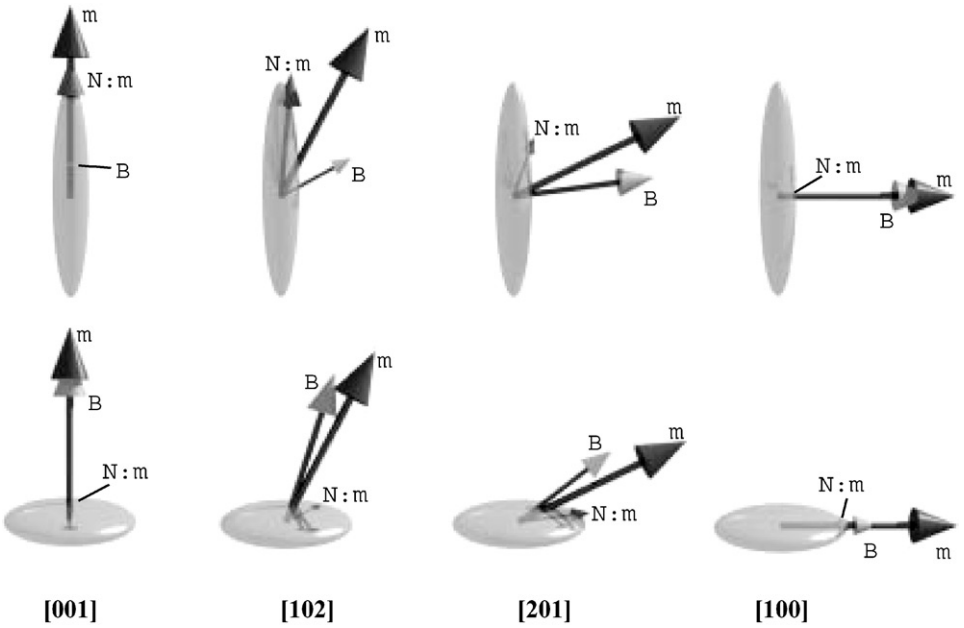

Fig. 3. Schematic representation of the relation between the unit magnetization vector $\hat{\mathbf{m}}$, the demagnetizing vector $\mathbf{H} = N : \hat{\mathbf{m}}$, and the resulting induction vector $\mathbf{B}$ for two different ellipsoid shapes: prolate (top row) and oblate (bottom row), and four different magnetization directions.

axes of order greater than 2 must have an isotropic N_{ij}. This does not mean that the tensor field itself is identical in all points. It means that all scalar quantities derived by contracting the tensor with respect to a vector are independent of the direction of that vector. In particular, this means that the magnetostatic energy Eq. (10) does not depend on the orientation of the magnetization vector for all of the Platonic and Archimedian particle shapes. This includes the tetrahedron and the cube. For all these particle shapes, the volume averaged, or magnetometric, demagnetization tensor is equal to that of the sphere, i.e., $\langle N_{ij} \rangle = \frac{1}{3}\delta_{ij}$.

4. Conclusions

In this paper, we have presented a new Fourier-space approach which allows us to calculate analytically the demagnetization tensor field for a broad class of magnetic nanoparticles. In particular, all the faceted (polyhedral) particles can be profitably described in Fourier space, thus obtaining a convenient way to compute quantities of interest in nanomagnetism, such as demagnetizing energy and field. The approach allows us also to investigate the class of rotational solids, and some solids with a high degree of symmetry, and further work is in progress to extend the computational scheme. The analytical solution for the demagnetization tensor field of the finite cylinder will be presented in a forthcoming publication.

In order to make progress in the research on magnetic materials, this theoretical framework must be tested against experiment and employed to measure physical quantities. Transmission electron microscopy experiments will be carried out in the near future with nanoparticles of well-defined geometry or magnetic structures of interest. Electron holography and related phase retrieval techniques may enable us to access the information regarding magnetic fields around the particles or structures. Such information would be suitable for a thorough comparison with the results of the calculations presented here.

From the micromagnetic point of view, the opportunity to calculate exactly the demagnetizing energy and field of uniformly magnetized cells of

any geometry (hexagonal plates, triangles or generic polyhedra for 3D computations), will represent a considerable improvement in the accuracy and speed of the simulations. Work in this direction is currently in progress.

Acknowledgements

The authors would like to acknowledge stimulating interactions with S. Tandon, J. Zhu, M. McHenry, D. Laughlin, and Y. Zhu. Financial support was provided by the U.S. Department of Energy, Basic Energy Sciences, under contract numbers DE-FG02-01ER45893 and DE-AC02-98CH10886.

References

[1] S. Chikazumi, Physics of Ferromagnetism, Oxford University Press, Oxford, 1997.
[2] H. Fukushima, Y. Nakatani, N. Hayashi, IEEE Trans. Magn. 34 (1998) 193.
[3] J. Komrska, Optik 80 (1987) 171.
[4] M. Beleggia, S. Tandon, Y. Zhu, M. De Graef, Philos. Mag. B 83 (2003) 1143.
[5] M. Beleggia, G. Pozzi, Phys. Rev. B 63 (2001) 4507.
[6] M. Beleggia, G. Pozzi, J. Masuko, N. Osakabe, K. Harada, T. Yoshida, O. Kamimura, H. Kasai, T. Matsuda, A. Tonomura, Phys. Rev. B 66 (2002) 4518.
[7] M. Beleggia, P.F. Fazzini, G. Pozzi, Ultramicroscopy (2003), in press.
[8] R. Moskowitz, E. Della Torre, IEEE Trans. Magn. 2 (1966) 739.
[9] M. Beleggia, Y. Zhu, Philos. Mag. B 83 (2003) 1043.
[10] M. Abramozitz, I. Stegun, Handbook of Mathematical Functions, Dover Publications Inc., New York, 1972.
[11] J. Komrska, W. Neumann, Phys. Stat. Sol. A 150 (1995) 89.
[12] Rayshade 4.0. http://graphics.stanford.edu/~cek/rayshade/rayshade.html.
[13] http://neon.mems.cmu.edu/degraef/tetrahedron.mpg.
[14] J.F. Nye, Physical Properties of Crystals, Clarendon Press, Oxford, 1964.
[15] A.S. Nowick, Crystal Properties via Group Theory, Cambridge University Press, Cambridge, 1995.